CELL-TYPE SPECIFIC PLASTICITY AT INTRAPALLIDAL SYNAPSES IN A MOUSE MODEL OF PARKINSON'S DISEASE

by

Kevin T. Zitelli

B.S., University of Pittsburgh 2013

Submitted to the Graduate Faculty of

The School of Medicine in partial fulfillment

of the requirements for the degree of M.S. in

Neurobiology

University of Pittsburgh

2016

UNIVERSITY OF PITTSBURGH

SCHOOL OF MEDICINE

This thesis was presented

by

Kevin T. Zitelli

It was defended on

August 11, 2016

and approved by

Aryn Gittis, Adjunct Assistant Professor, Neurobiology

Susanne Ahmari, Assistant Professor, Psychiatry

Robert Turner, Associate Professor, Neurobiology

Thesis Director: Aryn Gittis, Adjunct Assistant Professor, Neurobiology

CELL-TYPE SPECIFIC PLASTICITY AT INTRAPALLIDAL SYNAPSES IN A MOUSE MODEL OF PARKINSON'S DISEASE

Kevin T. Zitelli, B.S.

University of Pittsburgh, 2016

CELL-TYPE SPECIFIC PLASTICITY AT INTRAPALLIDAL SYNAPSES IN A MOUSE MODEL OF PARKINSON'S DISEASE

Kevin T. Zitelli, B.S.

University of Pittsburgh, 2016

Abstract

The cell types that comprise neural networks are critical in determining their function. Within the globus pallidus externa (GPe), a nucleus of the basal ganglia implicated in Parkinsonism, several neuronal subpopulations have been described genetically and anatomically, but functional and physiological studies have been limited. This study examines the previously undescribed collateral connections between two key cell types in the GPe, defined by the genetic expression of parvalbumin (PV) or LIM homeobox 6 (Lhx6). Further investigation of this network in a mouse model of Parkinson's Disease reveals a selective weakening of synaptic input from PV to Lhx6 neurons following dopamine lesions. This study builds on recent literature elucidating the roles of specific GPe cell types to basal ganglia function in health and disease.

TABLE OF CONTENTS

LIST OF FIGURES

1.0 INTRODUCTION

1.1 BASAL GANGLIA

The basal ganglia (BG) are a set of highly interconnected subcortical nuclei which, together, form a critical component of the motor structure within the central nervous system of vertebrates. The BG are central in a broad loop between the cortex and the thalamus, with information flowing from cortex, through the BG, and back to the cortex through the thalamus (Parent and Hazrati, 1995). These connections are thought to allow the BG to read and modify motor instructions before they are executed, participating in such processes as motor planning (Houk and Wise, 1995, Graybiel, 1998, Monchi et al., 2006) and action selection (Graybiel et al., 1994, Redgrave et al., 1999).

Several anatomically distinct nuclei comprise the BG, including the striatum, globus pallidus, subthalamic nucleus (STN), and substantia nigra. The globus pallidus and substantia nigra both can be further anatomically and functionally subdivided: the globus pallidus into the external (GPe) and internal (GPi) segments, and the substantia nigra into the pars compacta (SNc) and pars reticulata (SNr). Information in the BG is primarily received in the striatum and flows out through the GPi and SNr. The striatum projects to these output nuclei directly, but also projects to the GPe. Both the GPe and STN also innervate the BG output nuclei, in addition to being highly interconnected with one another.

Classically, the BG have been divided into two functionally opposing branches, known as the “direct” and “indirect” pathways. These pathways arise from two distinct types of striatal

projection neurons, known as medium spiny neurons (MSNs), marked genetically by the type of dopamine receptors they express. MSNs that express D2-type dopamine receptors project to the GPe, forming the first component of the indirect pathway, whereas D1-expressing MSNs bypass the GPe and project directly to BG output nuclei, comprising the direct pathway (Smith et al., 1998). Although both MSN types are GABAergic, and therefore inhibitory, the two pathways have opposing effects on BG output: D1-MSNs directly inhibit BG output nuclei, suppressing output, whereas D2-MSNs indirectly facilitate BG output by relieving the tonic inhibition of output nuclei by the GPe (Albin et al., 1989). Tonic inhibitory output from the GPi/SNr suppresses motor movements, serving as a kind of brake on motor activity (Deniau and Chevalier, 1985). Thus, the indirect pathway engages this brake, whereas the direct pathway relieves it. As such, dichotomous activation of one pathway or the other allows the BG to strongly influence which voluntary actions are carried out by an organism, and which are suppressed.

1.2 PARKINSON'S DISEASE

Parkinson's Disease (PD) is a progressive, neurodegenerative disease of the BG that afflicts approximately five million people worldwide (Olanow et al., 2009). Its cardinal symptoms are motor deficiencies, including bradykinesia, resting tremor, rigidity, postural instability, and shuffling gait (Jankovic, 2008). These symptoms indicate a general paucity of movement, and become debilitating to PD patients. Because current PD treatments have limited effectiveness and associated risks (Cotzias et al., 1969, Merims and Giladi, 2008), new treatments could improve patients' well-being. Since the BG is a primary brain area affected by

PD, a clearer understanding of how the normal role of the BG in movement is disrupted by PD could lead to new, and potentially more effective, treatment targets.

1.2.1 Role of dopamine in the striatum

PD is the result of the selective degeneration of dopamine (DA) neurons in the SNc, but the etiology is unclear. DA neurons of the SNc project broadly, targeting many areas of the brain, both within and outside of the BG (Guyenet and Aghajanian, 1978). However, among these numerous targets, DAergic innervation of the dorsal striatum is particularly dense (Descarries et al., 1996, Matsuda et al., 2009). As the dorsal region of the striatum is particularly involved in movement, loss of an important input to this area is a key factor in the development of motor symptoms in PD.

DAergic input to the striatum differentially modulates the D1- and D2-MSNs that form the starting points for the direct and indirect pathways. Both receptor types are coupled with G-proteins and have complex molecular interactions, but ultimately, their physiological effects oppose each other: D1 receptor activation enhances neuronal excitability, whereas D2 receptors diminish excitability (Neve et al., 2004). So, because striatal DAergic input serves to promote activity of the motor-enhacing direct pathway, and inhibits activity of the motor-suppressing indirect pathway, the overall effect of DA input to the striatum is pro-kinetic. As SNc neurons degenerate in PD, this pro-kinetic signal is lost. Under these conditions, the normal balance of activity between the direct and indirect pathways is disrupted. D1-MSNs are less active than in healthy conditions, and D2-MSNs are overactive (Albin et al., 1989, Mallet et al., 2006). The result is excessive BG output and suppression of movement, which is manifest in the motor symptoms of PD.

The resulting imbalance between the direct and indirect pathways that occurs after DA loss in PD is key to understanding the pathophysiology of the disease, but it is not the end of the story. DA replacement therapy, which restores the pro-kinetic signal to the striatum through drugs such as L-DOPA, is limited in its effectiveness due to adverse side effects, acquired drug resistance, and diminished potency as SNc neurons continue to degenerate (Cotzias et al., 1969, Merims and Giladi, 2008). Additionally, the effects of DA loss reach far beyond DA's action on D1 and D2 receptors. A slew of additional changes accompany chronic DA loss, altering the properties of the BG in ways that will be discussed in the following section.

1.2.2 GPe contributions to PD pathophysiology

Complex changes accompany the loss of DAergic input to MSNs, characteristically transforming the properties of the BG. Firing patterns become more irregular and/or bursty in several BG nuclei, including the GPe and GPi (Filion, 1979, Raz et al., 2000, Wichmann and Soares, 2006), STN (Levy et al., 2000, Wichmann and Soares, 2006), and SNr (Wichmann et al., 1999). Alongside these firing pattern changes is the aberrant intensification of oscillatory activity between 13-30 Hz, typically referred to as the β-frequency range (Hutchison et al., 1997, Hutchison et al., 1998, Brown et al., 2001). Although it is unclear that these oscillations are necessary for the development of motor deficits in PD, a correlation has been shown between the reduction of β-oscillations and the alleviation of PD symptoms during L-DOPA therapy (Kuhn et al., 2006). It has been suggested that the enhancement of this frequency range in the BG may occlude voluntary motor plans in favor of maintaining the current motor state, potentially explaining the difficulty in movement initiation seen in PD patients (Gilbertson et al., 2005, Engel and Fries, 2010, Little and Brown, 2014). Although amplified β-oscillations are found

throughout the Parkinsonian BG, their origin remains unknown. However, the centrality of the GPe in the BG circuit makes it ideally suited for the transmission of pathological activity throughout (Smith et al., 1998, Mallet et al., 2008, Connelly et al., 2010). Indeed, a number of prominent changes of the GPe and its connections have been identified as potential contributors to mechanisms of aberrant BG function.

Numerous studies suggest that aberrant GPe function contributes to PD pathophysiology in a variety of ways. A prominent hypothesis implicates recurrent GPe-STN connections in the facilitation of β-oscillations throughout the BG. The GPe-STN projection exerts powerful inhibitory control (Hallworth and Bevan, 2005, Baufreton et al., 2009), and becomes even more pronounced with the loss of DAergic neurons (Fan et al., 2012). After DA depletion, these reciprocally connected nuclei demonstrate reverberating, rhythmic activity in the β range, patterning each other's behavior (Plenz and Kital, 1999, Mallet et al., 2008, Atherton et al., 2013, Nevado-Holgado et al., 2014). When this reverberation is interrupted by pharmacologically blocking GPe input to the STN, β-oscillations are reduced, and Parkinsonian symptoms improve (Bergman et al., 1990, Wichmann et al., 1994, Tachibana et al., 2011). Deep brain stimulation of both the GPe (Vitek et al., 2004) and STN (Benabid et al., 1994, Limousin et al., 1995) also alleviate motor deficits. More recently, reciprocal connections between the GPe and striatum have also been hypothesized to contribute to aberrant BG function, though a causal role of these connections in PD pathophysiology has yet to be demonstrated (Mallet et al., 2012, Corbit et al., 2016, Glajch et al., 2016).

In health, the desynchronized and regular firing patterns of GPe neurons (DeLong et al., 1985, Nini et al., 1995) are shaped by their intrinsic properties, such as pace-making ability and lateral inhibition (Chan et al., 2004, Sadek et al., 2007, Goldberg et al., 2013, Wilson, 2013).

Changes to such intrinsic properties have been implicated in the emergence of abberant oscillations and irregularity following DA loss. Downregulation of hyperpolarization-activated cyclic nucleotide-gated channel expression weakens the pace-making ability of GPe neurons, contributing to the irregular firing patterns seen in Parkinsonism (Chan et al., 2011). A decline in $GABA_A$ receptor subunit expression has also been shown to follow DA lesions (Caruncho et al., 1997, Chadha et al., 2000). The lateral synaptic connections between GPe neurons may also play an important role in PD pathophysiology. Several computational studies have suggested that changes in this intrapallidal network could contribute to circuit-wide aberrant function in the BG (Terman et al., 2002, Goldberg et al., 2013, Wilson, 2013). It has been shown that synapses between GPe neurons are potentiated post-synaptically following DA lesions (Miguelez et al., 2012), potentially upsetting the balance of inhibition in the nucleus. Unfortunately, despite the complex and heterogeneous nature of the GPe-GPe network (Sadek et al., 2007), tools to study these connections on a microcircuit level have not existed until recently. Just as distinct cell types within the striatum have a defining role in the function of the nucleus, recent studies show that the GPe has similar genetic and functional cellular diversity. Before contributions of the intrapallidal network to PD pathophysiology can be fully understood, the dynamics of distinct cell types within the nucleus must be examined.

1.3 CELL TYPES OF THE GLOBUS PALLIDUS EXTERNA

Although classic models of the BG envisage the GPe as a uniform, intermediate relay nucleus, evidence of diverse cell types has been observed since the earliest investigation of pallidal function. Functional evidence of distinct neuronal subpopulations has been shown

consistently in electrophysiological recordings of behaving animals, with data demonstrating that GPe neurons display heterologous firing patterns in response to movement (DeLong, 1971, Jaeger et al., 1995, Turner and Anderson, 1997, Benhamou et al., 2012). Dichotomous physiologically-defined neuron types have also been observed in recordings of tonic GPe activity, with most neurons firing at a rapid, regular rate, and a smaller subset of neurons showing sparse, irregular activity (Mallet et al., 2008, Mallet et al., 2012, Abdi et al., 2015). Anatomical evidence has corroborated the division of the GPe into (at least) two distinct neuronal subpopulations. Fast, regular-firing "prototypic" GPe neurons project downstream to the STN and SNr, whereas the slow, irregular-firing "arkypallidal" neurons selectively target the striatum (Mallet et al., 2012). The physiological distinctions between these two classes of neurons are enhanced by DA loss, indicating that they may have differential roles in PD pathophysiology (Mallet et al., 2008, Mallet et al., 2012).

Many recent efforts have been made to establish genetic markers for GPe cell types, in order to better understand their functional differences, as well as to provide better tools to study them individually. Within the GPe, arkypallidal neurons uniquely express preproenkephalin (Mallet et al., 2012) and forkhead box protein P2 (FoxP2), whereas prototypic neurons are thought to be marked by the expression of the transcription factors NK2 homeobox 1 (Nkx2-1) and LIM homeobox 6 (Lhx6), and derive from a separate embryonic lineage (Dodson et al., 2015). Still further subdivisions of GPe cell types have been suggested, however. Genetic and anatomical studies have revealed that about 5% of GPe neurons express choline acetyltransferase exclusively of the markers proposed above (Mesulam et al., 1984, Rodrigo et al., 1998, Hernandez et al., 2015), and form a pathway between the GPe and frontal cortex whose role has yet to be thoroughly investigated (Saunders et al., 2015). Npas1 is also expressed by a minority

of GPe neurons, but since this population overlaps with markers of both prototypic and arkypallidal neurons, its usefulness as a label for a distinct class of GPe neurons is not yet clear (Hernandez et al., 2015). Finally, Mastro et. al 2014 provided evidence in adult transgenic mice that parvalbumin (PV) and Lhx6 mark functionally and anatomically distinct subclasses of prototypic GPe neurons. These two cell types differed in their intrinsic electrophysiological properties, and exhibited differential projection densities to areas both inside and outside of the BG, suggesting that they may serve distinct functional roles.

As efforts to categorize the roles of genetically distinct GPe cell types are relatively new, any contribution they may have to PD pathophysiology has barely been examined. Data of cell-type specific changes to GPe physiology are extremely limted. However, a study currently in review from our laboratory shows that differential modulation of PV and Lhx6-GPe neuron activity has a long-lasting pro-kinetic effect in a mouse model of PD (Mastro et al., 2016). When the GPe of bilaterally depleted mice were globally stimulated or inhibited, open-field motor activity did not change significantly. However, specific activation of PV-GPe (Fig. 1) and inhibition of Lhx6-GPe (Fig. 2) neurons both elicited robust and lengthy increases in motor behaviors. Though the mechanism for this effect is not clear, it is possible that the normal balance of activity between PV and Lhx6 neurons are shifted toward over-activation of Lhx6 neurons in the disease state, and that the inhibition of Lhx6 neurons either directly, or through activation of PV-GPe collaterals, rescues kinetic behavior. In support of this hypothesis, in-vivo recordings during optical activation show that a population of putative non-PV neurons is inhibited during PV-GPe stimulation (Fig. 3). These results suggest not only that these two cell types have differential behavioral roles, but also identify their interaction as a promising therapeutic target for PD.

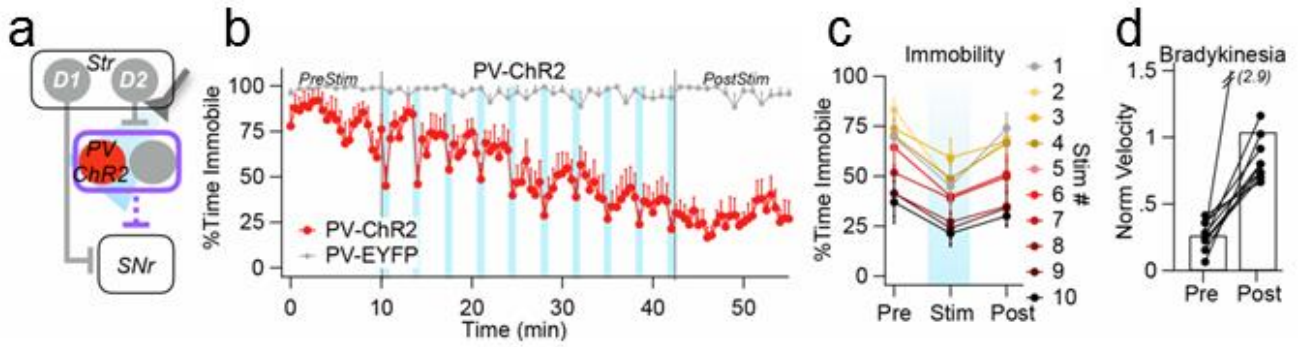

Figure 1. Selective stimulation of PV-GPe neurons rescues movement persistently in DA-depleted mice. (a) Schematic of optogenetic stimulation of PV-ChR2. **(b)** Percentage of time spent in the immobile state before, during and after stimulation. **(c)** Overlay of immobility immediately before (*pre)*, during (*stim)*, and after (*post*), each light pulse. **(d)** Movement velocities, normalized by naïve controls, before and after stimulation. Bars denote population averages; connected circles show data for individual mice.

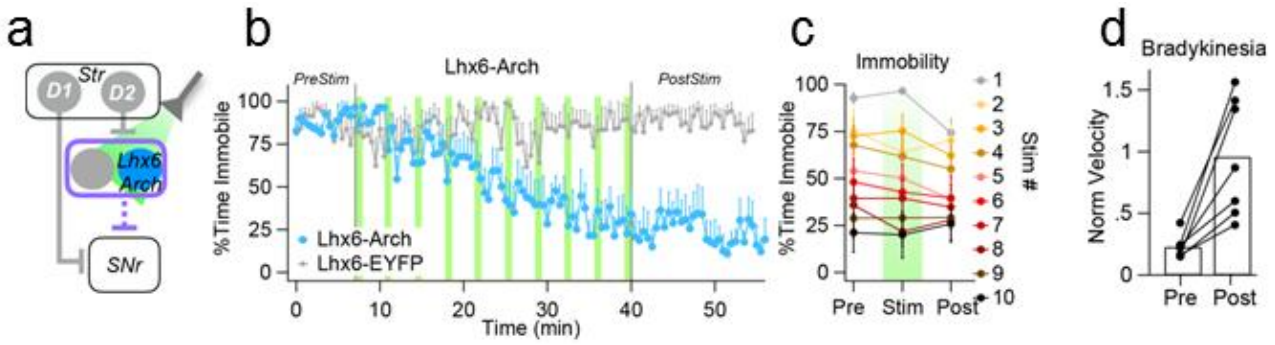

Figure 2. Selective inhibition of Lhx6-GPe neurons rescues movement persistently in DA-depleted mice. (a) Schematic of optogenetic inhibition of Lhx6-GPe neurons with archaerhodopsin. **(b)** Percentage of time spent in the immobile state before, during, and after inhibiton. **(c)** Overlay of immobility immediately before (*pre*), during (*stim*), and (*post*) each light pulse. **(d)** Movement velocities, normalized by naïve controls, before and after stimulation. Bars denote population averages; connected circles show data for individual mice.

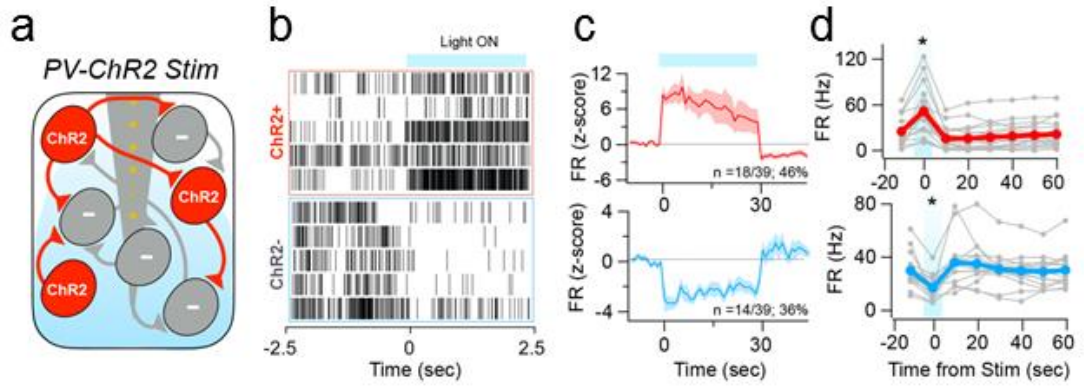

Figure 3. Network Response during PV-ChR2 stimulation. (a) Schematic of GPe network during PV-ChR2 stimulation. **(b)** Light evoked responses of ten single units during onset of a 30 sec light pulse. $ChR2^{+}$ denotes putative PV neurons, $ChR2^{-}$ denotes putative non-PV neurons. **(c)** Average z-score of excited (red, n = 18) and inhibited (blue, n =14) neurons during a 30 sec light pulse. Shaded area denoted standard error of the mean. **(d)** Firing rates of individual neurons before, during (time 0) and in 10 ms bins after a 30 sec light pulse. Population averages are shown as thick, colored lines.

1.4 EXPERIMENTAL GOALS

Microcircuits are critical in determining the overall function of nuclei, but given the novelty of genetically distinct GPe subpopulations, there has been little opportunity to examine intrapallidal circuit dynamics in a cell-type specific manner. Given the relevance of this network to BG function in health and disease, it is important to understand the individual contributions of specific cell types in both conditions. GPe-GPe synapses have previously been shown to be potentiated following DA lesions (Miguelez et al., 2012), but plasticity of distinct neuron types has not been examined. Changes in lateral inhibition between GPe neurons are thought to be relevant to PD pathophysiology (Goldberg et al., 2013, Schwab et al., 2013, Wilson, 2013), but whether these are global or specific has not been investigated. Our recent study using in-vivo optogenetics to modulate PV- and Lhx6-GPe neurons in a PD mouse model suggests that these two populations may be differentially affected by DA lesions.

In this study, the previously undescribed collateral connections between PV- and Lhx6-GPe are investigated. Using optogenetics with acute slice electrophysiology, the synaptic strength of the cell-type specific connections of both populations within the GPe are measured. Because no prior studies have examined the intrapallidal network in a cell-type specific manner, synaptic differences between the two neuronal subpopulations examined in this study were difficult to predict. However, based on a previous study showing a lower spontaneous firing rate of Lhx6 compared to PV-GPe neurons (Mastro et al., 2014), we reasoned that PV-Lhx6 synaptic connections may be more powerful than their reciprocal counterpart. Intrapallidal connections

are also examined in a mouse model of PD. Based on our previous behavioral results that the stimulation of PV-GPe and inhibition of Lhx6-GPe neurons are pro-kinetic following DA lesions, we believed a possible mechanism to be a shift in the relative dynamics of PV- and Lhx6-GPe activity toward over-activation of Lhx6-GPe neurons. Therefore, we hypothesized that intrapallidal inhibitory connections onto Lhx6 neurons are weakened after DA lesions. This study provides the first description of cell-type specific intrapallidal connections, and their potential role in PD pathophysiology.

2.0 MATERIALS AND METHODS

2.1 ANIMALS

Heterozygous mice on a C57BL/6J background were used for all experiments. Lhx6- and PV-GPe neurons were targeted for viral transfection using the Lhx6-iCre (Fogarty et al., 2007) or Pvalb-2A-Cre (Madisen et al., 2010) mouse lines. A subset of Pvalb-2A-Cre mice had also been crossed with an Lhx6-GFP mouse line (GENSAT, www.gensat.org) to allow for visualization of Lhx6-expressing neurons in these animals. Mice of both sexes were used in all groups. All experimental procedures were approved by the Carnegie Mellon University Institutional Animal Care & Use Committee, and are in accordance with the guidelines set forth by the National Institute of Health.

2.2 SURGICAL PROCEDURES

To achieve cell-specific expression of channelrhodopsin 2 (ChR2), the cre-dependent AAV2-DIO-ChR2-mCherry virus (University of North Carolina Vector Core Facility) was injected into the GPe of Lhx6-Cre, PV-Cre, or PV-Cre x Lhx6-GFP mice between the ages of 5-7 weeks. A mixture of ketamine (50 mg/mL) and xylazine (15 mg/mL) was administered intraperitoneally to induce anesthesia. After being placed in stereotaxic frame (Kopf

Instruments), anesthesia was maintained with 1.5% isofluorane during the course of the surgery. The scalp was opened, and holes drilled bilaterally into the skull above the GPe (0.17 mm anterior, 2.12 mm lateral of Bregma). A Nanoject (Drummond Scientific) with a pulled glass pipette tip was lowered 3.60 mm from the surface of the brain, and 300-400 nL of virus was injected into the GPe over the course of 4-5 minutes. After the completion of the injection, the pipette was allowed to remain in the brain for another five minutes, in order to prevent backflow of the virus. Once bilateral injections of the GPe had been made, the scalp was sutured, and the mouse was removed from the stereotaxic frame. After it recovered from anesthesia, the mouse was then returned to its home cage, and housed for 2-3 weeks to allow for expression of the virus.

A subset of animals were depleted of dopamine in a second surgery 11-18 days following their viral injection. These mice were anesthetized in the same way and placed on a stereotaxic frame. Holes were drilled bilaterally above the medial forebrain bundle (MFB, 0.45 mm posterior and 1.10 mm lateral of Bregma). A 33-guage cannula (Plastics One) was then positioned above the MFB, 5.10 mm below the surface of the brain. Five minutes after the cannula was positioned, 1μL of 6-hydroxydopamine (6OHDA, 5 μg/μL in 0.9% NaCl, Sigma) was injected at a rate of 0.2 μL/min. The cannula was then removed after five minutes. Following bilateral injections, the animal was sutured, and was returned to its home cage after recovery from anesthesia. To mitigate the deleterious health effects of bilateral dopamine depletion, special care was given to depleted animals. One half of their cage was placed on top of a heating pad, where it remained continually until the animal was sacrificed. Trail mix and soft, wet food, which was replaced daily, was placed inside the cage. Additionally, depleted animals

received a daily intraperitoneal injection of saline (0.9% NaCl). They were also monitored closely for excessive weight loss and other signs of distress.

2.3 ELECTROPHYSIOLOGICAL RECORDINGS

To prepare acute brain slices for patch-clamp electrophysiological recordings, mice between the ages of 7-10 weeks were sacrificed at least two weeks after viral injections, and their brains were sectioned parasagittally at a thickness of 300 μm. Mice that had been DA-depleted were sacrificed three days after being injected with 6-OHDA. Slices were prepared using a Leica VT1000S vibratome. During the slicing procedure, brain tissue was kept in carbogenated, ice-cold HEPES artificial cerebrospinal fluid consisting of the following (in mM): 20 HEPES, 92 NaCL, 1.2 $NaHCO_3$, 2.5 KCl, 10 $MgSO_4$, 0.5 $CaCl_2$, 30 NaH_2PO_4, 25 glucose, 5 sodium ascorbate, 2 thiourea, and 3 sodium pyruvate, at pH 7.3. Slices containing the GPe were transferred to a recovery solution at 33^oC for fifteen minutes, which contained the following (in mM): 93 *N*-methyl-D-glucamine, 2.5 KCl, 1.2 H_2PO_4, 30 $NaHCO_3$, 20 HEPES, 25 glucose, 10 $MgSO_4$, 0.5 $CaCl_2$, 5 sodium ascorbate, 2 thiourea, and 3 sodium pyruvate at pH 7.4. Following the recovery period, slices were transferred to a holding solution at room temperature and incubated for one hour before recording. The holding solution had the same components as the cutting solution, but contained 1 mM $MgCl_2$ and 2mM $CaCl_2$.

During recordings, slices were held at 33^oC in a bath of carbongenated artificial cerebrospinal fluid containing the following (in mM): 125 NaCl, 26 $NaHCO_3$, 1.25 NaH_2PO_4, 2.5 KCl, 12.5 glucose, 1 $MgCl_2$, and 2 $CaCl_2$. Electrodes were made from borosilicate glass (pipette resistance, 2-6 MΩ) and filled with an internal solution containing the following (in

mM): 120 $CsMeSO_3$, 15 CsCl, 8 NaCl, 0.5 EGTA, 10 HEPES, 2 Mg-ATP, 0.3 Na-GTP, 5 QX-314. Physiological recordings were made from individual neurons in the whole-cell voltage clamp configuration. Data were gathered using a Multiclamp 700B amplifier (Molecular Devices) and an ITC-18 analog-to-digital board (HEKA) with Igor Pro software (Wavemetrics) and Recording Artist acquisition code (Richard C. Gerkin, Phoenix).

2.4 IMMUNOHISTOCHEMISTRY

At the conclusion of electrophysiological recording, slices were fixed with 4% paraformaldehyde in phosphate-buffered saline solution (PBS) for 18-24 hours, then transferred to 30% sucrose in PBS for an additional 24 hours. Slices were then re-sectioned to a thickness of 30 μm prior to immunohistochemical processing. To stain for tyrosine hydroxylase (TH), re-sectioned tissue was incubated for 24 hours with primary rabbit anti-tyrosine hydroxylase antibody (1:1000, Pel-Freez), then washed and incubated for 1.5 hours with Alexa-Fluor-647 anti-rabbit (1:500, Invitrogen) secondary antibody. To quantify remaining TH in DA-lesioned animals, epifluorescent images were taken bilaterally in dorsal striatum at 10x magnification. Using the pixel intensity measuring tool in ImageJ, pixel intensity over a 75 x 75 μm area was measured from both hemispheres. These data were normalized against the same measurements made from parallel-processed tissue gathered from healthy control animals.

2.5 DATA ANALYSIS

Analysis of evoked inhibitory post-synaptic currents (IPSCs) was carried out using Igor Pro software (Wavemetrics). Group data were tested for normality using the Shapiro-Wilk test in SPSS (IBM). Because several group datasets were not normally distributed, non-parametric tests were used for statistical comparisons. Comparisons between cell types within the same group of animals were made using the Wilcoxon Signed Rank Test for paired data (WSRT). Any comparisons between groups were made using the Mann-Whitney Wilcoxon (MWW) test. For all statistical tests, significance levels were set at $\alpha = 0.05$. Throughout the text, data are reported as median ± standard deviation.

3.0 RESULTS

To examine cell-type specific synapses between GPe neurons, inhibitory post-synaptic currents (IPSCs) were optically evoked with ChR2 and recorded from GPe neurons of various types. Cell-type dependent expression of ChR2 was achieved by bilateral stereotaxic injections of AAV2-DIO-ChR2-mCherry into the GPe of Lhx6-Cre, PV-Cre, or PV-Cre x Lhx6-GFP animals 2-3 weeks prior to electrophysiological recordings. Brain slices used for recording were obtained from healthy control animals and DA-depleted animals 3 days after bilateral 6-OHDA injections into the MFB. To control variability, each slice was checked for viral expression by imaging for ChR2-mCherry prior to recording (Fig. 4A). Data were not gathered from slices that did not exhibit viral expression throughout the GPe. After recording, slices were immunohistochemically stained for TH. For DA-depleted animals, electrophysiological data were only used from slices that had less than 20% TH remaining in the dorsal striatum compared to healthy controls (Fig. 4B and 4C).

Voltage-clamp recordings were performed sequentially on neurons of heterogeneous types within 100 μm or each other. Cell types were primarily determined by ChR2 expression, which was tested by recording membrane currents at -80 mV while activating ChR2 with a 300 ms pulse of blue light. Neurons that showed a sustained current response during the latter part of the stimulation (100-300 ms) were considered $ChR2^{+}$, and assigned the cell type of PV or Lhx6 appropriately according to the genotype of the animal. Neurons that did not meet these criteria

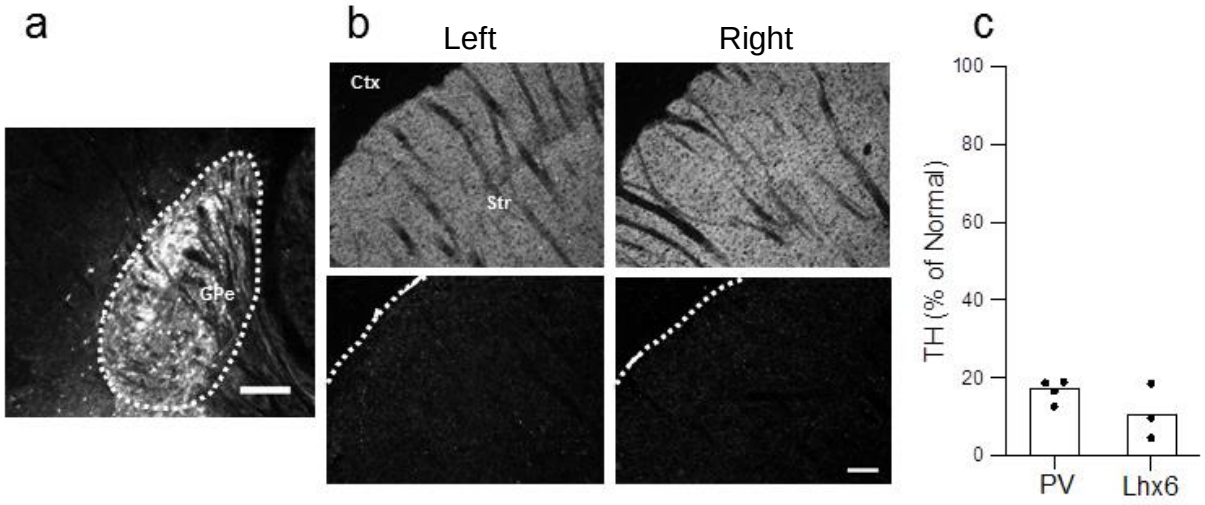

Figure 4. Histological verification of viral expression and TH immunoreactivity. (a) Epifluorescent image of viral expression in the GPe. Scale bar = 250 μm. **(b)** Representative images of striatal TH immunoreactivity in dorsal striatum of healthy control tissue (above) compared to a bilaterally depleted animal (below). Scale bar = 100 μm. **(c)** TH immunoreactivity, normalized to healthy controls, in bilaterally depleted PV-Cre and Lhx6-Cre animals. Bars denote population averages, dots denote data for individual animals.

were considered non-PV or non-Lhx6. In PV-Cre x Lhx6-GFP animals, neurons that were both $ChR2^-$ and GFP^+ were considered to be Lhx6 neurons (Fig. 5B).

IPSCs were recorded by evoking synaptic release with two 1 ms pulses of blue light 100ms apart. Cells were held at the reversal potential for ChR2 (0 mV) preclude ChR2-mediated currents (Nagel et al., 2003). IPSCs evoked by stimulation of Lhx6 neurons did not show a statistical difference in amplitude (Fig. 6C, n = 15, WSRT, p = 0.39) between responses from Lhx6 (1960 ± 679 pA) and non-Lhx6 neurons (1773 ± 733 pA). Similarly, IPSCs evoked by stimulation of PV neurons did not show a statistical difference in amplitude (Fig. 5, n = 20, WSRT, p = 0.87) between PV (1385 ± 963 pA) and non-PV neurons (1743 ± 609 pA), nor was there a difference between responses of PV and proximate Lhx6 neurons (Fig. 5D; PV-PV: 1217 ± 552 pA, PV-Lhx6: 1538 ± 562 pA; n = 5, WSRT, p = 0.44). Additionally, PV-evoked (n = 40, 1632 ± 795 pA) and Lhx6-evoked (n = 30, 1826 ± 714 pA) IPSC amplitudes were not significantly different (Fig. 7B, MWW, p = 0.43). These data suggest that there are no cell-type specific differences in the synaptic strength of intrapallidal collaterals in healthy mice. These results are not consistent with our hypothesis that Lhx6-GPe neurons receive stronger intrapallidal inhibitory input than PV-GPe neurons.

Results from DA-depleted tissue indicate that intrapallidal synaptic transmission had been altered in a cell-type specific manner relative to control conditions. When PV-GPe neurons were stimulated in DA-lesioned tissue, IPSCs in PV neurons (1345 ± 698 pA) and non-PV neurons (548 ± 415 pA) differed significantly (Fig. 5D, n = 34, WSRT, $p < 10^{-7}$). This difference held when comparing to the subset of non-PV neurons that were identified as Lhx6 (PV-PV: 1389 ± 788 pA, PV-Lhx6: 425 ± 475 pA; n = 21, WSRT, $p < 10^{-5}$). On the other hand, IPSCs evoked by Lhx6-GPe stimulation did not differ significantly (Fig. 6C, n = 18, MWW, p = 0.55)

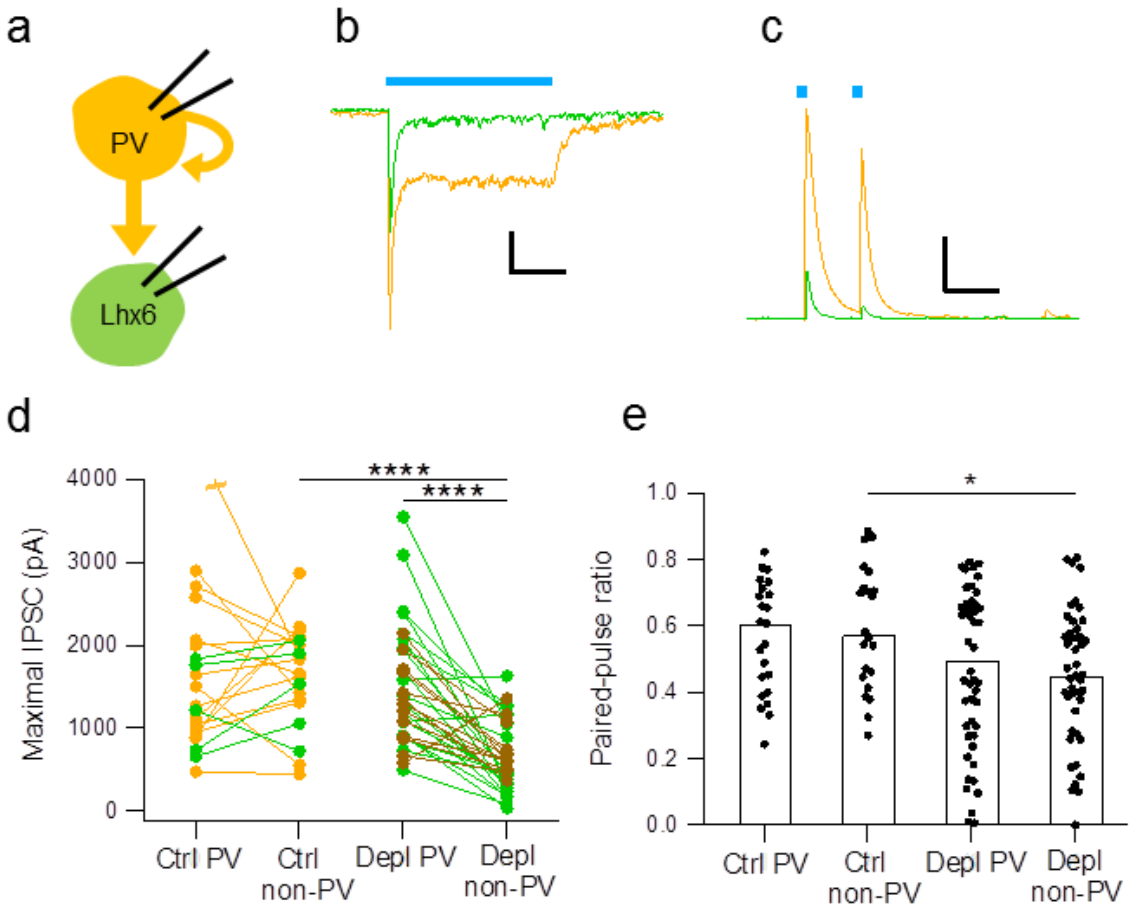

Figure 5. IPSCs in the GPe evoked by PV-GPe optogenetic stimulation. (a) Schematic of voltage clamp recordings in the GPe. PV-GPe terminals in the field of view were optogenetically stimulated while IPSCs were sequentially recorded in proximate PV (orange) and Lhx6 (green) or otherwise non-PV (not pictured) neurons. **(b)** Example current traces of $ChR2^+$ (orange) and $ChR2^-$ (green) neurons in response to 300 ms light pulse (blue bar). Scale bars denote 500 pA (vertical) and 100 ms (horizontal). **(c)** Example current traces of PV (orange) and Lhx6 (green) neurons in response to 1 ms light pulses (blue bars) in DA-depleted tissue. Scale bar denotes 500 pA (vertical) and 100 ms (horizontal). **(d)** Maximal IPSCs evoked by PV-GPe stimulation. Connected dots denote responses from proximate pairs of PV and non-PV neurons. Green pairs denote responses in which the non-PV neurons was identified as $Lhx6^+$. Asterisks indicate significance. **(e)** PPR of evoked IPSCs. Dots denote data for individual neurons; bars denote population medians. Asterisks indicate significance.

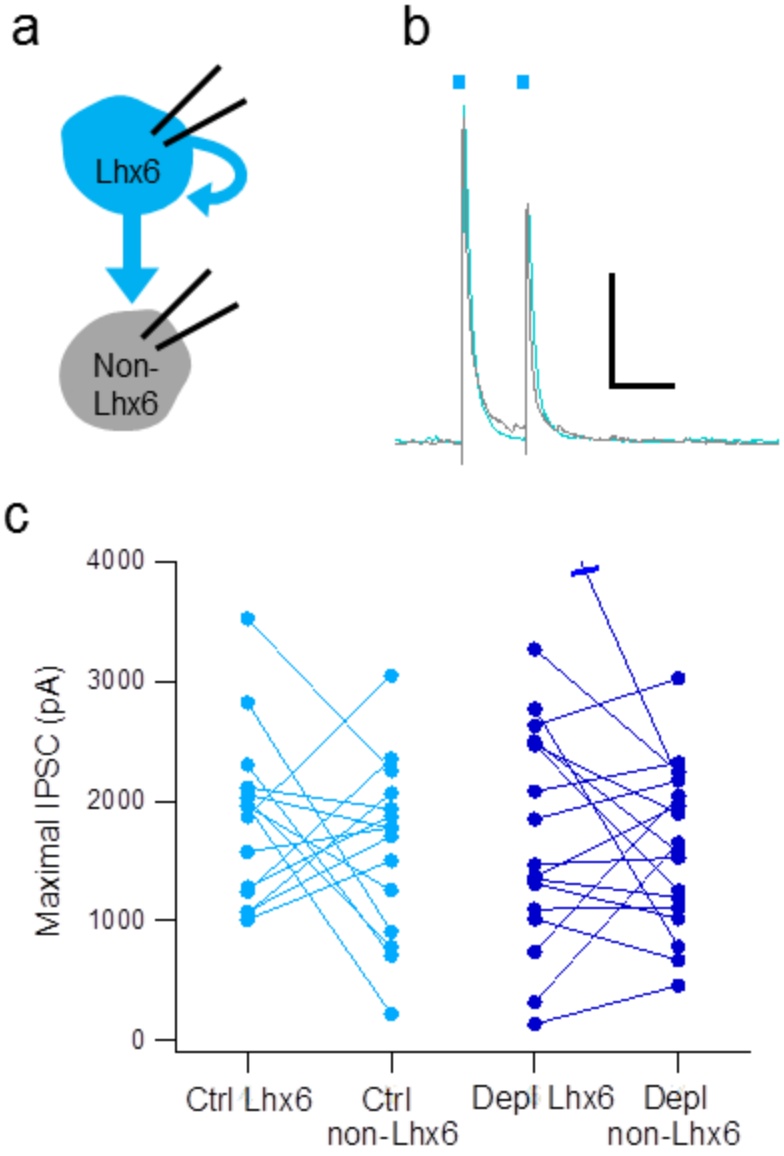

Figure 6. IPSCs in the GPe evoked by Lhx6-GPe optogenetic stimulation. (a) Schematic of voltage clamp recordings in the GPe. Lhx6-GPe terminals in the field of view were optogenetically stimulated while IPSCs were sequentially recorded in proximate Lhx6 (blue) and non-Lhx6 (gray) neurons. **(b)** Example current traces of PV (orange) and Lhx6 (green) neurons in response to 1 ms light pulses (blue bars) in DA-depleted tissue. Scale bar denotes 500 pA (vertical) and 100 ms (horizontal). **(d)** Maximal IPSCs evoked by Lhx6-GPe stimulation. Connected dots denote responses from proximate pairs of Lhx6 and non-Lhx6 neurons.

between Lhx6 (1661 ± 1150 pA) and non-Lhx6 neurons (1613 ± 675 pA). Furthermore, the decrease in IPSC amplitude observed in non-PV neurons was found to be statistically significant when compared to control conditions (Fig. 5D, MWW, $p < 10^{-7}$), which again held for PV-Lhx6 synaptic responses (MWW, $p < 10^{-6}$). Other synaptic responses were unchanged by DA-depletion, however. PV-PV IPSCs were similar in control and DA-depleted tissue (Fig. 7B, WSRT, $p = 0.83$), as were overall IPSC responses to Lhx6-stimulation (DA-depleted: n = 36, 1613 ± 938 pA; MWW, $p = 0.97$). These data suggest that, following DA loss, synaptic input from PV- to Lhx6-GPe neurons are weakened, while other intrapallidal connections among these neuron types remain unchanged. This result supports our hypothesis that intrapallidal inhibitory connections onto Lhx6 neurons are weakened after DA lesions.

To examine the mechanism for the decrease in PV-nonPV IPSC amplitude seen in DA-depleted animals, the paired-pulse ratio (PPR) of evoked IPSC amplitudes were compared across cell types and conditions. In control tissue, the PPR of responses in PV (0.61 ± 0.17) and non-PV (0.57 ± 0.18) did not differ significantly (Fig. 5E, MWW, $p = 0.60$). PPR was lower in both cell types in DA-lesioned tissue (PV: 0.50 ± 0.24, non-PV: 0.45 ± 0.20), but this decrease was only significant in non-PV neurons (Fig. 5E, MWW, PV: $p = 0.15$; non-PV: $p = 0.02$). These results do not explain the weakened response to PV stimulation seen in non-PV neurons following DA lesions. Typically, a decrease in PPR reflects an enhanced probability of synaptic release, a mechanism of synaptic potentiation (Schulz et al., 1994). The fact that decreased PPR accompanies the depressed responses seen at PV-nonPV synapses in DA-lesioned tissue suggests that other mechanisms of synaptic depression are responsible for the decreased IPSC amplitudes. Further study will be necessary to understand the mechanism of the plasticity demonstrated in these experiments.

In summary, our data show that while intrapallidal synaptic connections are similar across cell types in healthy conditions, PV input to Lhx6 neurons is selectively weakened after DA loss. These results support our hypothesis that intrapallidal inhibitory input to Lhx6 neurons is weakened in after DA lesions. Examination of the PPR at these synapses suggests that synaptic release probability may be enhanced, which does not explain the decrease in response amplitude. Further study will necessary to understand the mechanism of the plasticity demonstrated here, as well as its role in PD pathophysiology.

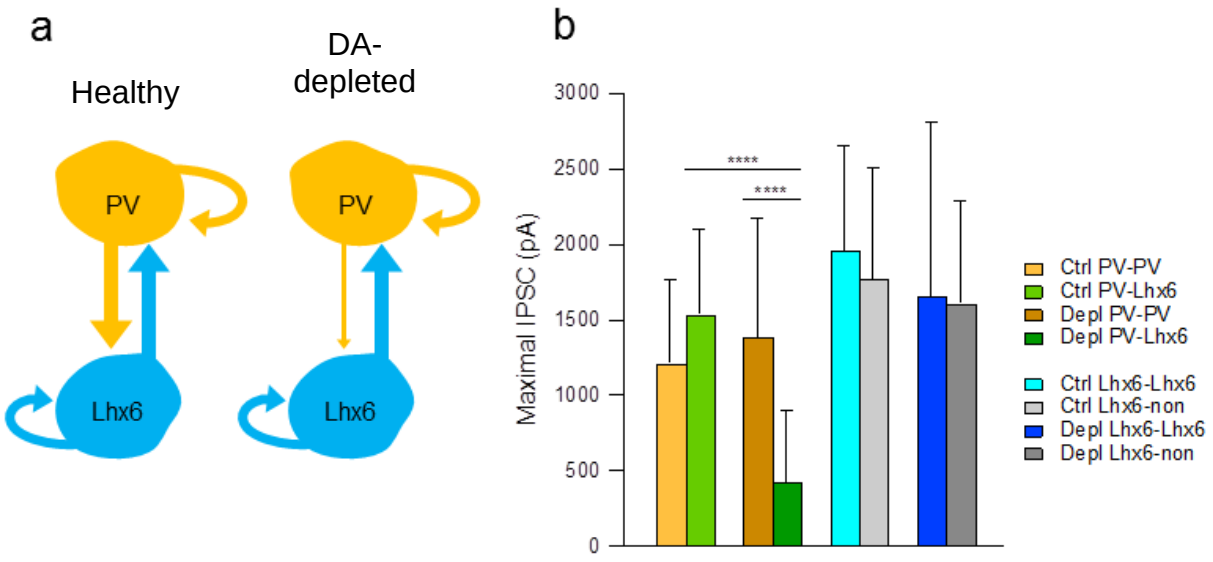

Figure 7. Summary of intrapallidal synaptic connections in healthy and DA-depleted tissue. (a) Schematic of intrapallidal synaptic connections. In health (left), lateral inhibition between PV and Lhx6 neurons is homogeneous. After DA-depletion (right), PV-Lhx6 input is selectively decreased. **(b)** Population data for maximal IPSCs across all conditions. Columns denote population medians. Error bars indicate standard deviation. Asterisks indicate significance.

4.0 DISCUSSION

This study provides the first characterization of intrapallidal synaptic transmission between two neuronal subpopulations of the GPe. Using the transgenic mouse lines PV-Cre and Lhx6-Cre, each population was independently stimulated with the use of optogenetics. This study revealed that while the connections between and within these two cell populations were essentially homogeneous in health, synaptic input from PV to Lhx6 neurons was selectively weakened in a mouse model of PD. These results reveal a putative cell-type specific contribution of the GPe to PD pathophysiology, and, with a further study, a new potential therapeutic target.

The decreased synaptic input from PV to Lhx6 neurons after DA loss were consistent with our hypothesis that intrapallidal inhibition onto Lhx6 neurons is weakened following DA depletion. This hypothesis was based on our previous study of the effects of in-vivo optogenetic stimulation of these same GPe cell types, which revealed that stimulation of PV neurons and inhibition of Lhx6 neurons both produced long-lasting pro-kinetic effects in the same mouse model of PD employed in the present study. Taken together, the results of these two studies suggest that in PD, Lhx6-GPe neurons receive insufficient intrapallidal inhibitory input, and restoring that inhibition, either directly or indirectly through PV collaterals, has a therapeutic effect on Parkinsonian motor symptoms. There are a few caveats to this interpretation, however. First, such a conclusion ignores input to the GPe from other sources, as well as differential output of these two cell types, which may also contribute to the therapeutic effect seen in our in-

vivo study. These factors will need to be investigated further. Next, while in the double transgenic PV-Cre x Lhx6-GFP mouse line, the PV and Lhx6 neuronal populations in the GPe barely overlap (Mastro et al., 2014), our more recent study shows that the PV-Cre and Lhx6-Cre populations overlap substantially (Mastro et al., 2016), in concurrence with other genetic studies of GPe subpopulations (Dodson et al., 2015, Hernandez et al., 2015). While these populations may not be mutually exclusive, they do not overlap entirely, and our differential synaptic and behavioral results strongly suggest that we are optically stimulating divergent cell populations. In future studies, alternative genetic tools, such as the PV-Flp mouse line (Madisen et al., 2015), may allow more selective optogenetic manipulation of these two cell populations.

Previous studies of intrapallidal synaptic transmission are limited. Our results differ from another study of intrapallidal synapses, which showed that IPSCs evoked by global GPe stimulation were potentiated, rather than depressed, by chronic DA-depletion. Numerous methodological differences may have contributed to this discrepancy. In the present study, DA-depletions were bilateral, and carried out 3 days prior to recording. We used this Parkinsonian model specifically so that we could examine the state of the GPe under same conditions as our previous study of in-vivo optogenetic modulation of GPe cell types. This is a notable difference from Miguelez et al. 2012, in which depletions were unilateral, and executed 2-3 weeks before recording; a much more chronic depletion by comparison. This difference in time course is the most likely reason for the differing conclusions between the studies; mechanisms of synaptic plasticity and compensation can operate on a timeline that exceeds 3 days. Because Miguelez et al. 2012 employed global GPe stimulation, rather than cell-type specific stimulation, it is not entirely certain that our results are wholly contradictory. To test this, our study would have to be repeated using a similar DA-depletion paradigm. It is possible, for instance, that PV-Lhx6

synapses are still weakened 2-3 weeks after DA-lesions, but other intrapallidal synapses are strengthened. Such a result would be masked by the global GPe stimulation utilized in Miguelez et al. 2012. For the moment, it is not possible for us to test whether the global nature of DA-depletion paradigm directly contributed to the difference between these studies. Our acute bilateral depletions were limited to 3 days because this procedure had severe deleterious effects on the health of the animal. It would be extremely unlike for a mouse acutely, bilaterally depleted in the manner described in this study to survive for 2 weeks. However, in the future, gradual DA-depletion models, such as the one described in (Willard et al., 2015), may obviate this problem after further characterization.

The mechanism for the altered transmission at PV-Lhx6 synapses remains unclear. Comparison of PPR data at this synapse between healthy and DA-depleted conditions suggested that presynaptic release probability was enhanced, rather than diminished, after DA-lesions. However, such a conclusion may not be entirely reliable. Previous studies have shown that stimulation of AAV2-ChR2 evoke artificially depressed responses compared to electrical stimulation at some synapses, though not all (Zhang and Oertner, 2007, Jackman et al., 2014). Alternate viral vectors for ChR2 have yielded improvement in this area, however (Jackman et al., 2014), so these may be useful in future cell-type specific studies of intrapallidal synapses. Of course, other mechanisms of plasticity may be at play at the PV-Lhx6 synapse. Previous studies of gene expression in the GPe have shown a downregulation of $GABA_A$-receptor subunits following DA lesions (Caruncho et al., 1997, Chadha et al., 2000). It is not clear that these receptors are downregulated specifically at intrapallidal synapses, but since striato-pallidal synaptic transmission is unchanged by DA-depletion (Miguelez et al., 2012), this would be a likely explanation. Furthermore, this downregulation of inhibitory receptors has been shown to

occur on a time course similar to the depletion paradigm used in this study (Caruncho et al., 1997). Examining cell-type specific expression of $GABA_A$ receptors in the GPe of DA-intact and depleted tissue might enable a firmer conclusion regarding the mechanism of plasticity at PV-Lhx6 synapses in the GPe. Other electrophysiological experiments, such as recording asynchronous synaptic release with the use of strontium, or measuring miniature IPSCs, would also be useful in assessing potential mechanisms of synaptic plasticity.

Numerous aspects of the GPe microcircuit have yet to be characterized. In health, PV and Lhx6-GPe neurons have differential intrinsic properties, including input resistance, capacitance, and spontaneous firing rate (Mastro et al., 2014), but the properties of these cell types have not been investigated in DA-depleted animals. GPe subpopulations have also been posited to differentially innervate targets both within and outside the BG (Bevan et al., 1998, Mastro et al., 2014, Saunders et al., 2015, Glajch et al., 2016). These projections have not been fully characterized in health, and have barely been examined in PD models. Innervation of the GPe by striatum and STN has also yet to be studied in a cell-type specific manner. These gaps in knowledge provide a multitude of future directions for investigations of the role of GPe subpopulations in PD pathophysiology.

In conclusion, this study provides the first cell-type specific characterization of lateral inhibition within the GPe, and demonstrates an alteration of synaptic input onto a particular neuronal subpopulation within the GPe in a mouse model of PD. These results may reveal an important aspect of the mechanism by which aberrant GPe activity arises in PD, and contributes to its pathophysiology. Considered along with data from another recent study in which GPe cell types were optogenetically modulated in-vivo in the same PD model (Mastro et al., 2016), the

results of the present study suggest that the synaptic alteration shown herein can be successfully targeted to alleviate Parkinsonian motor deficits.

BIBLIOGRAPHY

Abdi A, Mallet N, Mohamed FY, Sharott A, Dodson PD, Nakamura KC, Suri S, Avery SV, Larvin JT, Garas FN, Garas SN, Vinciati F, Morin S, Bezard E, Baufreton J, Magill PJ (2015) Prototypic and arkypallidal neurons in the dopamine-intact external globus pallidus. J Neurosci 35:6667-6688.

Albin RL, Young AB, Penney JB (1989) The functional anatomy of basal ganglia disorders. Trends Neurosci 12:366-375.

Atherton JF, Menard A, Urbain N, Bevan MD (2013) Short-term depression of external globus pallidus-subthalamic nucleus synaptic transmission and implications for patterning subthalamic activity. J Neurosci 33:7130-7144.

Baufreton J, Kirkham E, Atherton JF, Menard A, Magill PJ, Bolam JP, Bevan MD (2009) Sparse but selective and potent synaptic transmission from the globus pallidus to the subthalamic nucleus. J Neurophysiol 102:532-545.

Benabid AL, Pollak P, Gross C, Hoffmann D, Benazzouz A, Gao DM, Laurent A, Gentil M, Perret J (1994) Acute and long-term effects of subthalamic nucleus stimulation in Parkinson's disease. Stereotact Funct Neurosurg 62:76-84.

Benhamou L, Bronfeld M, Bar-Gad I, Cohen D (2012) Globus Pallidus external segment neuron classification in freely moving rats: a comparison to primates. PLoS One 7:e45421.

Bergman H, Wichmann T, DeLong MR (1990) Reversal of experimental parkinsonism by lesions of the subthalamic nucleus. Science 249:1436-1438.

Bevan MD, Booth PA, Eaton SA, Bolam JP (1998) Selective innervation of neostriatal interneurons by a subclass of neuron in the globus pallidus of the rat. J Neurosci 18:9438-9452.

Brown P, Oliviero A, Mazzone P, Insola A, Tonali P, Di Lazzaro V (2001) Dopamine dependency of oscillations between subthalamic nucleus and pallidum in Parkinson's disease. J Neurosci 21:1033-1038.

Caruncho HJ, Liste I, Rozas G, Lopez-Martin E, Guerra MJ, Labandeira-Garcia JL (1997) Time course of striatal, pallidal and thalamic alpha 1, alpha 2 and beta 2/3 GABAA receptor subunit changes induced by unilateral 6-OHDA lesion of the nigrostriatal pathway. Brain Res Mol Brain Res 48:243-250.

Chadha A, Dawson LG, Jenner PG, Duty S (2000) Effect of unilateral 6-hydroxydopamine lesions of the nigrostriatal pathway on GABA(A) receptor subunit gene expression in the rodent basal ganglia and thalamus. Neuroscience 95:119-126.

Chan CS, Glajch KE, Gertler TS, Guzman JN, Mercer JN, Lewis AS, Goldberg AB, Tkatch T, Shigemoto R, Fleming SM, Chetkovich DM, Osten P, Kita H, Surmeier DJ (2011) HCN channelopathy in external globus pallidus neurons in models of Parkinson's disease. Nat Neurosci 14:85-92.

Chan CS, Shigemoto R, Mercer JN, Surmeier DJ (2004) HCN2 and HCN1 channels govern the regularity of autonomous pacemaking and synaptic resetting in globus pallidus neurons. J Neurosci 24:9921-9932.

Connelly WM, Schulz JM, Lees G, Reynolds JN (2010) Differential short-term plasticity at convergent inhibitory synapses to the substantia nigra pars reticulata. J Neurosci 30:14854-14861.

Corbit VL, Whalen TC, Zitelli KT, Crilly SY, Rubin JE, Gittis AH (2016) Pallidostriatal Projections Promote beta Oscillations in a Dopamine-Depleted Biophysical Network Model. J Neurosci 36:5556-5571.

Cotzias GC, Papavasiliou PS, Gellene R (1969) L-dopa in parkinson's syndrome. N Engl J Med 281:272.

DeLong MR (1971) Activity of pallidal neurons during movement. J Neurophysiol 34:414-427.

DeLong MR, Crutcher MD, Georgopoulos AP (1985) Primate globus pallidus and subthalamic nucleus: functional organization. J Neurophysiol 53:530-543.

Deniau JM, Chevalier G (1985) Disinhibition as a basic process in the expression of striatal functions. II. The striato-nigral influence on thalamocortical cells of the ventromedial thalamic nucleus. Brain Res 334:227-233.

Descarries L, Watkins KC, Garcia S, Bosler O, Doucet G (1996) Dual character, asynaptic and synaptic, of the dopamine innervation in adult rat neostriatum: a quantitative autoradiographic and immunocytochemical analysis. J Comp Neurol 375:167-186.

Dodson PD, Larvin JT, Duffell JM, Garas FN, Doig NM, Kessaris N, Duguid IC, Bogacz R, Butt SJ, Magill PJ (2015) Distinct developmental origins manifest in the specialized encoding of movement by adult neurons of the external globus pallidus. Neuron 86:501-513.

Engel AK, Fries P (2010) Beta-band oscillations--signalling the status quo? Curr Opin Neurobiol 20:156-165.

Fan KY, Baufreton J, Surmeier DJ, Chan CS, Bevan MD (2012) Proliferation of external globus pallidus-subthalamic nucleus synapses following degeneration of midbrain dopamine neurons. J Neurosci 32:13718-13728.

Filion M (1979) Effects of interruption of the nigrostriatal pathway and of dopaminergic agents on the spontaneous activity of globus pallidus neurons in the awake monkey. Brain Res 178:425-441.

Fogarty M, Grist M, Gelman D, Marin O, Pachnis V, Kessaris N (2007) Spatial genetic patterning of the embryonic neuroepithelium generates GABAergic interneuron diversity in the adult cortex. J Neurosci 27:10935-10946.

Gilbertson T, Lalo E, Doyle L, Di Lazzaro V, Cioni B, Brown P (2005) Existing motor state is favored at the expense of new movement during 13-35 Hz oscillatory synchrony in the human corticospinal system. J Neurosci 25:7771-7779.

Glajch KE, Kelver DA, Hegeman DJ, Cui Q, Xenias HS, Augustine EC, Hernandez VM, Verma N, Huang TY, Luo M, Justice NJ, Chan CS (2016) Npas1+ Pallidal Neurons Target Striatal Projection Neurons. J Neurosci 36:5472-5488.

Goldberg JA, Atherton JF, Surmeier DJ (2013) Spectral reconstruction of phase response curves reveals the synchronization properties of mouse globus pallidus neurons. J Neurophysiol 110:2497-2506.

Graybiel AM (1998) The basal ganglia and chunking of action repertoires. Neurobiol Learn Mem 70:119-136.

Graybiel AM, Aosaki T, Flaherty AW, Kimura M (1994) The basal ganglia and adaptive motor control. Science 265:1826-1831.

Guyenet PG, Aghajanian GK (1978) Antidromic identification of dopaminergic and other output neurons of the rat substantia nigra. Brain Res 150:69-84.

Hallworth NE, Bevan MD (2005) Globus pallidus neurons dynamically regulate the activity pattern of subthalamic nucleus neurons through the frequency-dependent activation of postsynaptic GABAA and GABAB receptors. J Neurosci 25:6304-6315.

Hernandez VM, Hegeman DJ, Cui Q, Kelver DA, Fiske MP, Glajch KE, Pitt JE, Huang TY, Justice NJ, Chan CS (2015) Parvalbumin+ Neurons and Npas1+ Neurons Are Distinct Neuron Classes in the Mouse External Globus Pallidus. J Neurosci 35:11830-11847.

Houk JC, Wise SP (1995) Distributed modular architectures linking basal ganglia, cerebellum, and cerebral cortex: their role in planning and controlling action. Cereb Cortex 5:95-110.

Hutchison WD, Allan RJ, Opitz H, Levy R, Dostrovsky JO, Lang AE, Lozano AM (1998) Neurophysiological identification of the subthalamic nucleus in surgery for Parkinson's disease. Ann Neurol 44:622-628.

Hutchison WD, Lozano AM, Tasker RR, Lang AE, Dostrovsky JO (1997) Identification and characterization of neurons with tremor-frequency activity in human globus pallidus. Exp Brain Res 113:557-563.

Jackman SL, Beneduce BM, Drew IR, Regehr WG (2014) Achieving high-frequency optical control of synaptic transmission. J Neurosci 34:7704-7714.

Jaeger D, Gilman S, Aldridge JW (1995) Neuronal activity in the striatum and pallidum of primates related to the execution of externally cued reaching movements. Brain Res 694:111-127.

Jankovic J (2008) Parkinson's disease: clinical features and diagnosis. J Neurol Neurosurg Psychiatry 79:368-376.

Kuhn AA, Kupsch A, Schneider GH, Brown P (2006) Reduction in subthalamic 8-35 Hz oscillatory activity correlates with clinical improvement in Parkinson's disease. Eur J Neurosci 23:1956-1960.

Levy R, Hutchison WD, Lozano AM, Dostrovsky JO (2000) High-frequency synchronization of neuronal activity in the subthalamic nucleus of parkinsonian patients with limb tremor. J Neurosci 20:7766-7775.

Limousin P, Pollak P, Benazzouz A, Hoffmann D, Le Bas JF, Broussolle E, Perret JE, Benabid AL (1995) Effect of parkinsonian signs and symptoms of bilateral subthalamic nucleus stimulation. Lancet 345:91-95.

Little S, Brown P (2014) The functional role of beta oscillations in Parkinson's disease. Parkinsonism Relat Disord 20 Suppl 1:S44-48.

Madisen L, Garner AR, Shimaoka D, Chuong AS, Klapoetke NC, Li L, van der Bourg A, Niino Y, Egolf L, Monetti C, Gu H, Mills M, Cheng A, Tasic B, Nguyen TN, Sunkin SM, Benucci A, Nagy A, Miyawaki A, Helmchen F, Empson RM, Knopfel T, Boyden ES, Reid RC, Carandini M, Zeng H (2015) Transgenic mice for intersectional targeting of neural sensors and effectors with high specificity and performance. Neuron 85:942-958.

Madisen L, Zwingman TA, Sunkin SM, Oh SW, Zariwala HA, Gu H, Ng LL, Palmiter RD, Hawrylycz MJ, Jones AR, Lein ES, Zeng H (2010) A robust and high-throughput Cre reporting and characterization system for the whole mouse brain. Nat Neurosci 13:133-140.

Mallet N, Ballion B, Le Moine C, Gonon F (2006) Cortical inputs and GABA interneurons imbalance projection neurons in the striatum of parkinsonian rats. J Neurosci 26:3875-3884.

Mallet N, Micklem BR, Henny P, Brown MT, Williams C, Bolam JP, Nakamura KC, Magill PJ (2012) Dichotomous organization of the external globus pallidus. Neuron 74:1075-1086.

Mallet N, Pogosyan A, Marton LF, Bolam JP, Brown P, Magill PJ (2008) Parkinsonian beta oscillations in the external globus pallidus and their relationship with subthalamic nucleus activity. J Neurosci 28:14245-14258.

Mastro KJ, Bouchard RS, Holt HA, Gittis AH (2014) Transgenic mouse lines subdivide external segment of the globus pallidus (GPe) neurons and reveal distinct GPe output pathways. J Neurosci 34:2087-2099.

Mastro KJ, Zitelli KT, Willard AM, Leblanc KH, Kravitz AV, Gittis AH (2016) Cell-Specific Pallidal Intervention Induces Long-Lasting Motor Recovery in Dopamine Depleted mice. In Review.

Matsuda W, Furuta T, Nakamura KC, Hioki H, Fujiyama F, Arai R, Kaneko T (2009) Single nigrostriatal dopaminergic neurons form widely spread and highly dense axonal arborizations in the neostriatum. J Neurosci 29:444-453.

Merims D, Giladi N (2008) Dopamine dysregulation syndrome, addiction and behavioral changes in Parkinson's disease. Parkinsonism Relat Disord 14:273-280.

Mesulam MM, Mufson EJ, Levey AI, Wainer BH (1984) Atlas of cholinergic neurons in the forebrain and upper brainstem of the macaque based on monoclonal choline acetyltransferase immunohistochemistry and acetylcholinesterase histochemistry. Neuroscience 12:669-686.

Miguelez C, Morin S, Martinez A, Goillandeau M, Bezard E, Bioulac B, Baufreton J (2012) Altered pallido-pallidal synaptic transmission leads to aberrant firing of globus pallidus neurons in a rat model of Parkinson's disease. J Physiol 590:5861-5875.

Monchi O, Petrides M, Strafella AP, Worsley KJ, Doyon J (2006) Functional role of the basal ganglia in the planning and execution of actions. Ann Neurol 59:257-264.

Nagel G, Szellas T, Huhn W, Kateriya S, Adeishvili N, Berthold P, Ollig D, Hegemann P, Bamberg E (2003) Channelrhodopsin-2, a directly light-gated cation-selective membrane channel. Proc Natl Acad Sci U S A 100:13940-13945.

Nevado-Holgado AJ, Mallet N, Magill PJ, Bogacz R (2014) Effective connectivity of the subthalamic nucleus-globus pallidus network during Parkinsonian oscillations. J Physiol 592:1429-1455.

Neve KA, Seamans JK, Trantham-Davidson H (2004) Dopamine receptor signaling. J Recept Signal Transduct Res 24:165-205.

Nini A, Feingold A, Slovin H, Bergman H (1995) Neurons in the globus pallidus do not show correlated activity in the normal monkey, but phase-locked oscillations appear in the MPTP model of parkinsonism. J Neurophysiol 74:1800-1805.

Olanow CW, Stern MB, Sethi K (2009) The scientific and clinical basis for the treatment of Parkinson disease (2009). Neurology 72:S1-136.

Parent A, Hazrati LN (1995) Functional anatomy of the basal ganglia. I. The cortico-basal ganglia-thalamo-cortical loop. Brain Res Brain Res Rev 20:91-127.

Plenz D, Kital ST (1999) A basal ganglia pacemaker formed by the subthalamic nucleus and external globus pallidus. Nature 400:677-682.

Raz A, Vaadia E, Bergman H (2000) Firing patterns and correlations of spontaneous discharge of pallidal neurons in the normal and the tremulous 1-methyl-4-phenyl-1,2,3,6-tetrahydropyridine vervet model of parkinsonism. Journal of Neuroscience 20:8559-8571.

Redgrave P, Prescott TJ, Gurney K (1999) The basal ganglia: a vertebrate solution to the selection problem? Neuroscience 89:1009-1023.

Rodrigo J, Fernandez P, Bentura ML, de Velasco JM, Serrano J, Uttenthal O, Martinez-Murillo R (1998) Distribution of catecholaminergic afferent fibres in the rat globus pallidus and their relations with cholinergic neurons. J Chem Neuroanat 15:1-20.

Sadek AR, Magill PJ, Bolam JP (2007) A single-cell analysis of intrinsic connectivity in the rat globus pallidus. J Neurosci 27:6352-6362.

Saunders A, Oldenburg IA, Berezovskii VK, Johnson CA, Kingery ND, Elliott HL, Xie T, Gerfen CR, Sabatini BL (2015) A direct GABAergic output from the basal ganglia to frontal cortex. Nature 521:85-89.

Schulz PE, Cook EP, Johnston D (1994) Changes in paired-pulse facilitation suggest presynaptic involvement in long-term potentiation. J Neurosci 14:5325-5337.

Schwab BC, Heida T, Zhao Y, Marani E, van Gils SA, van Wezel RJ (2013) Synchrony in Parkinson's disease: importance of intrinsic properties of the external globus pallidus. Front Syst Neurosci 7:60.

Smith Y, Bevan MD, Shink E, Bolam JP (1998) Microcircuitry of the direct and indirect pathways of the basal ganglia. Neuroscience 86:353-387.

Tachibana Y, Iwamuro H, Kita H, Takada M, Nambu A (2011) Subthalamo-pallidal interactions underlying parkinsonian neuronal oscillations in the primate basal ganglia. Eur J Neurosci 34:1470-1484.

Terman D, Rubin JE, Yew AC, Wilson CJ (2002) Activity patterns in a model for the subthalamopallidal network of the basal ganglia. J Neurosci 22:2963-2976.

Turner RS, Anderson ME (1997) Pallidal discharge related to the kinematics of reaching movements in two dimensions. J Neurophysiol 77:1051-1074.

Vitek JL, Hashimoto T, Peoples J, DeLong MR, Bakay RA (2004) Acute stimulation in the external segment of the globus pallidus improves parkinsonian motor signs. Mov Disord 19:907-915.

Wichmann T, Bergman H, DeLong MR (1994) The primate subthalamic nucleus. III. Changes in motor behavior and neuronal activity in the internal pallidum induced by subthalamic inactivation in the MPTP model of parkinsonism. J Neurophysiol 72:521-530.

Wichmann T, Bergman H, Starr PA, Subramanian T, Watts RL, DeLong MR (1999) Comparison of MPTP-induced changes in spontaneous neuronal discharge in the internal pallidal segment and in the substantia nigra pars reticulata in primates. Exp Brain Res 125:397-409.

Wichmann T, Soares J (2006) Neuronal firing before and after burst discharges in the monkey basal ganglia is predictably patterned in the normal state and altered in parkinsonism. J Neurophysiol 95:2120-2133.

Willard AM, Bouchard RS, Gittis AH (2015) Differential degradation of motor deficits during gradual dopamine depletion with 6-hydroxydopamine in mice. Neuroscience 301:254-267.

Wilson CJ (2013) Active decorrelation in the basal ganglia. Neuroscience 250:467-482.

Zhang YP, Oertner TG (2007) Optical induction of synaptic plasticity using a light-sensitive channel. Nat Methods 4:139-141.